

Observation of the decay mode $K_L \rightarrow \pi^+\pi^-e^+e^-$

Y. Takeuchi, Y. Hemmi¹, H. Kurashige², Y. Matono,
K. Murakami, T. Nomura³, H. Sakamoto, N. Sasao, M. Suehiro

Department of Physics, Kyoto University, Kyoto 606-8502, Japan

Y. Fukushima, Y. Ikegami, T. T. Nakamura, T. Taniguchi

High Energy Accelerator Research Organization (KEK), Ibaraki 305-0801, Japan

M. Asai

Hiroshima Institute of Technology, Hiroshima 731-5193, Japan

Abstract

We report on results of an experimental search for the $K_L \rightarrow \pi^+\pi^-e^+e^-$ decay mode. We found 13.5 ± 4.0 events and determined its branching ratio to be $(4.4 \pm 1.3(\text{stat.}) \pm 0.5(\text{syst.})) \times 10^{-7}$. The result agrees well with the theoretical prediction.

PACS: 13.20.Eb, 14.40.Aq

1 Introduction

In the previous Letter [1], we reported the results of our experimental search for the decay mode $K_L \rightarrow \pi^+\pi^-e^+e^-$, which established the upper limit of 4.6×10^{-7} (90% CL) on its branching ratio. In this decay mode, CP violation may occur as an interference between two intermediate states with different CP properties [2,3]. Thus it can provide a new testing ground for investigating CP violation. A theoretical model predicts a branching ratio of about 3×10^{-7} [2]. Encouraged by this value, we continued the experiment further aiming to

¹ Present address: *Daido Institute of Technology, Aichi 457, Japan*

² Present address: *Kobe University, Hyogo 657-8501, Japan*

³ Contact person: nomurat@scphys.kyoto-u.ac.jp

establish this decay mode. Recently a group at the Fermilab (KTeV) reported the measurement of its branching ratio based on 36.6 ± 6.8 observed events [4]. In this article, we present our new result [5].

The experiment was conducted with a 12-GeV proton synchrotron at High Energy Accelerator Research Organization (KEK). The experimental set-up, shown in Fig. 1, was already described in Ref. [1]. We used the same set-up with one vital change: the decay volume, which had been filled with helium gas in the preceding run, was evacuated down to 8×10^{-3} Torr. As will be seen, this was very effective to reduce backgrounds originating from nuclear interactions. Below we briefly describe our set-up for convenience. The K_L

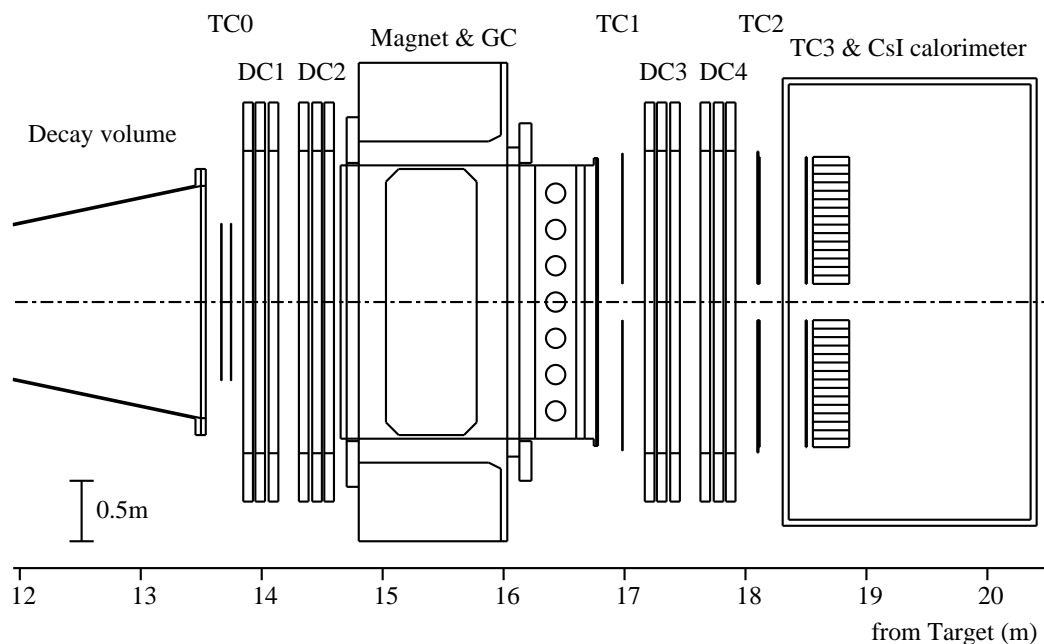


Fig. 1. Schematic plan view of the KEK-E162 detector

beam was produced by focusing 12-GeV/c primary protons onto a 60-mm-long copper target. The divergence of neutral beam was ± 4 mrad horizontally and ± 20 mrad vertically. Following the 4-m-long decay volume was a charged particle spectrometer. It consisted of four sets of drift chambers (DC1-DC4) and an analyzing magnet with an average horizontal momentum kick of 136 MeV/c. The drift chamber position resolution was in average $210 \mu\text{m}$, and its efficiency was greater than 98% under a typical running condition. A threshold Cherenkov counter (GC) with pure N_2 gas at 1 atm was placed inside of the magnet gap to identify electrons. For the present decay mode, we obtained, by adjusting software cuts in the off-line analysis, an average electron efficiency of 99.7% with a pion-rejection factor of 50. Two banks of pure CsI electromagnetic calorimeters, located at the far end, measured energy and position

of electrons and photons. Its energy and position resolutions were found to be approximately 3% and 7 mm for 1-GeV electrons, respectively. There were 4 sets of trigger scintillation counters, called TC0X, TC1X, TC2X/2Y and TC3X, where X(Y) represented a horizontally(vertically)-segmented hodoscope. The trigger for the present mode was designed to select events with at least three charged tracks which included at least two electrons.

2 General Analysis and Normalization Mode

In order to exploit full statistical power of the available data, we combined the present data (vacuum data) with the one presented in Ref. [1] (He data), and analyzed them without distinction. Approximate K_L flux ratio of the vacuum to He data set was 5 : 1. We closely followed the off-line analysis procedure described in Ref. [1] with refinements at several places. At first, events were required to have 4 (and only 4) tracks with a common vertex in the beam region inside the decay volume. Then particle species were determined. A pion was identified as a track which could project onto a cluster in the calorimeter (a matched track) with $E/p < 0.7$, where E and p were an energy deposit measured by the calorimeter and a momentum of the track determined by the spectrometer, respectively. An electron was identified as a matched track with $E \geq 200$ MeV, $0.9 \leq E/p \leq 1.1$, and GC hits in the corresponding cells. The events containing π^+ , π^- , e^+ and e^- tracks were selected, and then applied two kinematical cuts. One was the requirement for the invariant mass of e^+e^- pair (M_{ee}) to be at least 4 MeV/ c^2 ; this cut was effective to suppress backgrounds from external conversion of γ -rays into e^+e^- pair. The other was a limit on the pion momentum asymmetry ($A_{+-} \equiv (p_{\pi^+} - p_{\pi^-}) / (p_{\pi^+} + p_{\pi^-})$) within ± 0.5 . This cut was introduced in Ref. [1] to suppress backgrounds due to nuclear interactions, but was found also useful to remove events with pion decays. The remaining events are our basic event samples for further analysis, and mainly contain both signal mode $K_L \rightarrow \pi^+\pi^-e^+e^-$ and normalization mode $K_L \rightarrow \pi^+\pi^-\pi^0$ ($\pi^0 \rightarrow e^+e^-\gamma$).

We now identify the normalization mode (denoted as $\pi^+\pi^-\pi_D^0$ in the following). We required at least one γ -ray with energy above 200 MeV. Here a γ -ray was defined as a cluster in the calorimeter which did not match with any charged tracks. If more than one γ -ray existed, we selected the one for which the invariant mass of $e^+e^-\gamma$ ($M_{ee\gamma}$) was closest to the π^0 mass. Then we imposed three major kinematical cuts to select $\pi^+\pi^-\pi_D^0$ events. First, the invariant mass of $e^+e^-\gamma$ ($M_{ee\gamma}$) was required to be within $3\sigma_{M_{\pi^0}}$ of the π^0 mass (M_{π^0}), where the π^0 mass resolution $\sigma_{M_{\pi^0}}$ was measured to be 4.6 MeV/ c^2 . Second, θ^2 was required to be less than 20 mrad², where θ denotes the angle of the reconstructed K_L momentum with respect to the line connecting the production target and decay vertex. Fig. 2 shows the invariant mass dis-

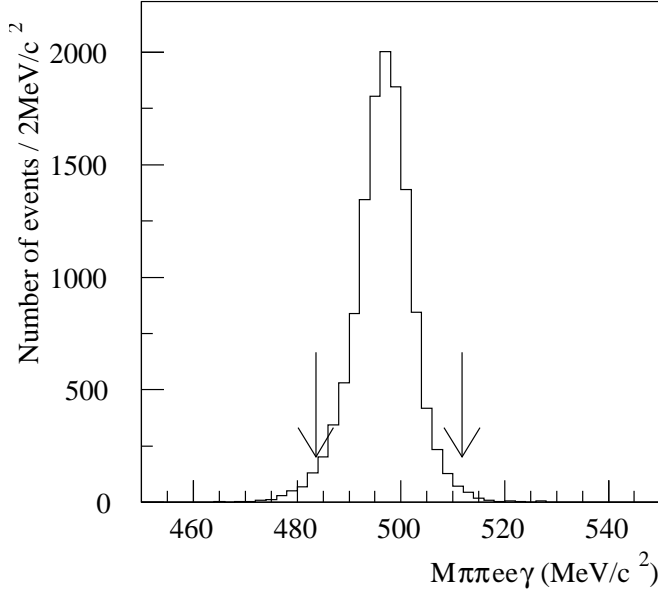


Fig. 2. The invariant mass distribution of $\pi^+\pi^-e^+e^-\gamma$. The arrows indicate the region to select the $K_L \rightarrow \pi^+\pi^-\pi_D^0$ events.

tribution of $\pi^+\pi^-e^+e^-\gamma$ ($M_{\pi\pi ee\gamma}$) for the events which satisfied all the cuts mentioned so far. A clear K_L peak can be seen with a mass resolution ($\sigma_{M_{K_L}}$) of 5.5 MeV/c². As a final cut, events were requested to lie within $3\sigma_{M_{K_L}}$ of the K_L mass (M_{K_L}). After all the cuts, 12212 events remained [6]. We call these events the $\pi^+\pi^-\pi_D^0$ reconstructed events.

3 Signal Mode and Background Subtraction

For the signal mode $K_L \rightarrow \pi^+\pi^-e^+e^-$, the major backgrounds came from $\pi^+\pi^-\pi_D^0$ events with an extra γ -ray missed from detection. We employed the same strategy as in Ref. [1]. At first, we removed events which had extra γ -ray(s) consistent with $\pi^0 \rightarrow e^+e^-\gamma$. To reduce the data set size, we also applied at this stage loose kinematical cuts; $\theta^2 \leq 100 \text{ mrad}^2$ and $410 < M_{\pi\pi ee} < 590 \text{ MeV}/c^2$, where $M_{\pi\pi ee}$ being the invariant mass of $\pi^+\pi^-e^+e^-$. Then we defined a parameter which quantified consistency of an event with $\pi^+\pi^-\pi_D^0$. The parameter, called χ_D^2 , was given by

$$\chi_D^2(\vec{p}_\gamma) = \left(\frac{M_{ee\gamma} - M_{\pi^0}}{\sigma_{M_{\pi^0}}} \right)^2 + \left(\frac{M_{\pi\pi ee\gamma} - M_{K_L}}{\sigma_{M_{K_L}}} \right)^2 + \left(\frac{\theta}{\sigma_\theta} \right)^2,$$

where \vec{p}_γ was an arbitrary momentum of a γ -ray assumed to exist [7]. The standard deviations $\sigma_{M_{\pi^0}}$, $\sigma_{M_{K_L}}$ and σ_θ [8] were all obtained from the $\pi^+\pi^-\pi_D^0$

reconstructed events. We determined \vec{p}_γ by minimizing χ_D^2 . Fig. 3 shows the

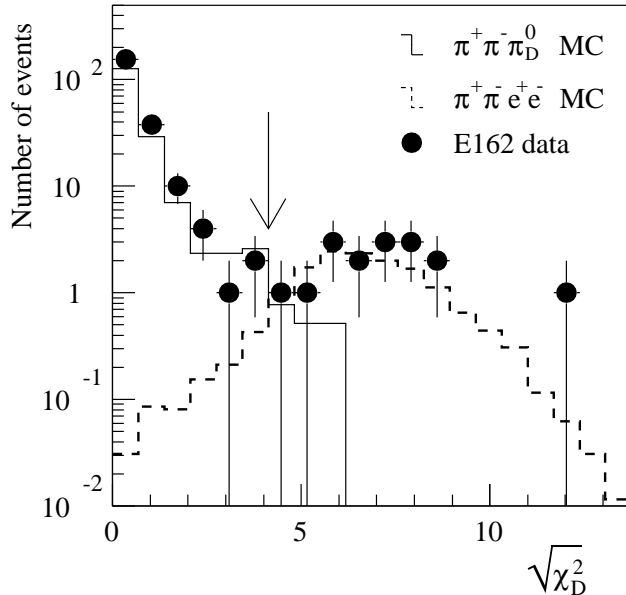


Fig. 3. The distribution of the square root of χ_D^2 . The solid and dashed lines are the results of Monte Carlo (MC) simulation, respectively, for the $\pi^+\pi^-\pi_D^0$ and $\pi^+\pi^-e^+e^-$ modes. The K_L flux in the simulations was normalized with the reconstructed $\pi^+\pi^-\pi_D^0$ events, and the branching ratio for $\pi^+\pi^-e^+e^-$ was assumed to be given by our final result. The arrow shows the cut position.

$\sqrt{\chi_D^2}$ distribution of the events after minimization. (Here only the events with $\theta^2 \leq 20 \text{ mrad}^2$ and $|M_{\pi\pi ee} - M_{K_L}| < 5\sigma_{M_{K_L}}$ are plotted to illustrate clearly existence of two components.) The solid and dashed lines in the figure show the results of Monte Carlo (MC) simulations, respectively, for the $\pi^+\pi^-\pi_D^0$ and $\pi^+\pi^-e^+e^-$ modes. The K_L flux in the simulations was normalized with the reconstructed $\pi^+\pi^-\pi_D^0$ events, and the branching ratio for $\pi^+\pi^-e^+e^-$ was assumed to be given by our final result. We considered the events with $\chi_D^2 < 17$ as $\pi^+\pi^-\pi_D^0$ events, and removed from the sample. The cut rejected 99.7% of the $\pi^+\pi^-\pi_D^0$ background, while retaining 92% of the signal. Fig. 4(a) shows the $M_{\pi\pi ee}$ vs θ^2 scatter plot of the $\pi^+\pi^-e^+e^-$ candidate events after the χ_D^2 cut. Here the solid dots represent the vacuum data and the plus the He data. Let us first consider the vacuum data. We notice that there exists a cluster of events (15 events) inside our signal box defined by $\theta^2 \leq 20 \text{ mrad}^2$ and $|M_{\pi\pi ee} - M_{K_L}| < 3\sigma_{M_{K_L}}$. Fig. 4(b) is the corresponding plot obtained by the $\pi^+\pi^-\pi_D^0$ MC simulation. Note that the MC statistics in the plot is about 5 times more than the vacuum data. We also notice that there are non-negligible backgrounds remaining similarly in both plots. They are more or less uniformly distributed along the θ^2 -direction, and form two distinct bands. It is found from the MC study that there exist two mechanisms for the $\pi^+\pi^-\pi_D^0$ events to pass through the χ_D^2 cut. One is γ -radiation: events in which e^+/e^- radiates

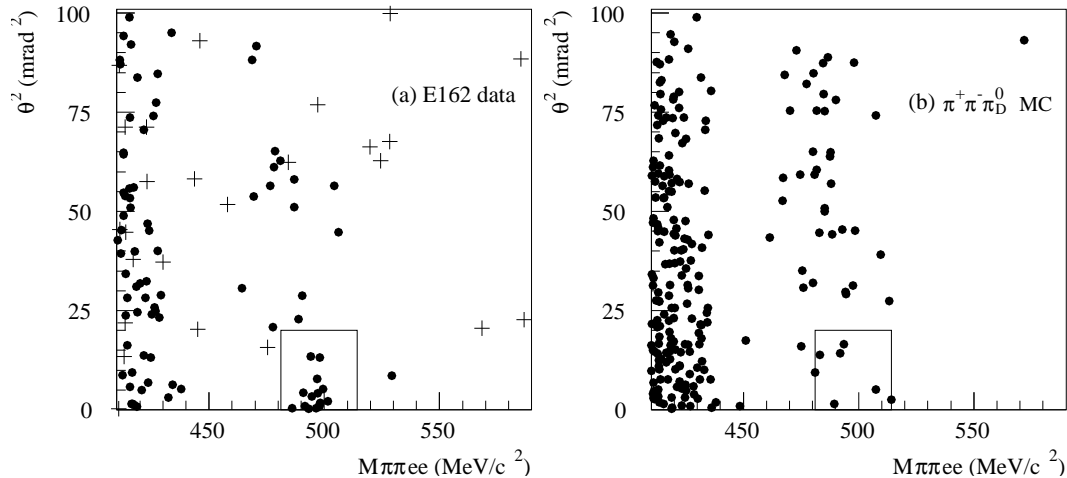


Fig. 4. (a) The $M_{\pi\pi ee}$ vs θ^2 scatter plot of the $K_L \rightarrow \pi^+\pi^-e^+e^-$ candidate events after the χ_D^2 cut. The solid dots represent the vacuum data and the plus the He data. The box indicates the signal region. (b) The corresponding scatter plot obtained by the $\pi^+\pi^-\pi_D^0$ MC simulation. Note that the MC statistics is 5 times more than the vacuum data.

γ -rays internally or externally would lose its energy. Such events constitute the low mass background band. The other is π -decay: events in which π^+/π^- decays inside the magnet would have wrong momentum assignment. The high mass backgrounds are due mainly to these events. Next we consider the He data. There is no event left inside the signal box [9], as was reported in Ref. [1]. The backgrounds outside the signal box are spread more broadly compared with the vacuum data. These events are most probably due to the nuclear interactions off the helium nucleus.

We now want to estimate the number of backgrounds inside the signal box. To this end, we relied upon the fact that, for both He and vacuum data, the background distribution was approximately flat along the θ^2 -axis. We thus projected the events with $|M_{\pi\pi ee} - M_{K_L}| < 3\sigma_{M_{K_L}}$ onto the θ^2 -axis. The resultant distribution is shown in Fig. 5. There is a clear signal peak at $\theta^2 = 0$. The solid line in the figure represents the $\pi^+\pi^-\pi_D^0$ MC simulation, in which the K_L flux was normalized with the reconstructed $\pi^+\pi^-\pi_D^0$ events. We defined a ‘‘control’’ region to be $30 < \theta^2 < 100$ mrad². We then determined a scale factor by normalizing the number of $\pi^+\pi^-\pi_D^0$ MC events in this region (5.2 events) to that of the data (6 events). The number of backgrounds was given by the number of $\pi^+\pi^-\pi_D^0$ MC events in the signal region (1.3 events) times the scale factor (1.15). We found this to be 1.5 ± 1.0 , where the error includes uncertainty due to the MC statistics. Subtracting this from the events inside the signal box, we determined the number of signal events to be 13.5 ± 4.0 .

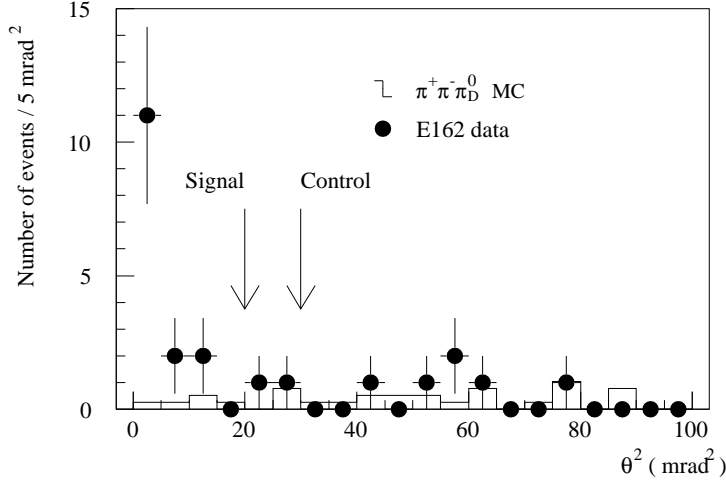


Fig. 5. The θ^2 projection of the $K_L \rightarrow \pi^+\pi^-e^+e^-$ candidate events. The solid line in the figure represents the $\pi^+\pi^-\pi_D^0$ MC simulation. Its K_L flux was normalized by the reconstructed $\pi^+\pi^-\pi_D^0$ events. The arrows indicate the signal and control region boundaries.

4 Branching Ratio and Systematic Errors

The branching ratio was calculated by

$$Br(K_L \rightarrow \pi^+\pi^-e^+e^-) = Br(K_L \rightarrow \pi^+\pi^-\pi_D^0) \times Br(\pi_D^0 \rightarrow e^+e^-\gamma) \\ \times \frac{A(\pi^+\pi^-\pi_D^0)}{A(\pi^+\pi^-e^+e^-)} \cdot \frac{\eta(\pi^+\pi^-\pi_D^0)}{\eta(\pi^+\pi^-e^+e^-)} \cdot \frac{N(\pi^+\pi^-e^+e^-)}{N(\pi^+\pi^-\pi_D^0)}$$

where A , η and N denote acceptance, efficiency and observed number of events, respectively. The detector acceptances were determined by MC simulations, and were found to be 0.98×10^{-3} for $\pi^+\pi^-\pi_D^0$ and 2.6×10^{-3} for $\pi^+\pi^-e^+e^-$ [10]. Here, the latter acceptance depends upon the $\pi^+\pi^-e^+e^-$ matrix elements; we employed a theoretical model given by Ref. [2]. Most of efficiencies were common to the both modes, and they tended to cancel out in the efficiency ratio. The largest difference stemmed from the detection efficiency of extra γ -rays in $\pi^+\pi^-\pi_D^0$. Using a MC simulation, we estimated its inefficiency to be 20.4%. The χ_D^2 cut and $\pi_D^0 \rightarrow e^+e^-\gamma$ inclusive cut were applied only to the signal mode: the efficiency of the former was found to be 92% while the over-veto due to the latter was estimated to be 1%. We found that all other effects caused negligibly small difference in the ratio of efficiency. Using the known branching ratio of $Br(K_L \rightarrow \pi^+\pi^-\pi_D^0) = 0.1256$ and $Br(\pi_D^0 \rightarrow e^+e^-\gamma) = 1.198 \times 10^{-2}$ [11], we finally arrived at the branching ratio of

$$Br(K_L \rightarrow \pi^+\pi^-e^+e^-) = (4.4 \pm 1.3 \pm 0.5) \times 10^{-7},$$

Table 1

Summary of systematic errors in the branching ratio.

Source	uncertainty
K_L momentum spectrum	4.8%
Matrix element	3.9%
Others	3.1%
Background subtraction	7.4%
Nuclear interaction	3.6%
Other contamination	1.4%
$Br(K_L \rightarrow \pi^+ \pi^- \pi_D^0)$	3.1%
Total	11.3%

where the first (second) error represents the statistical (systematic) uncertainty.

Table 1 summarizes our systematic errors, which are divided into three categories. The first one is related to the acceptance-efficiency ratio. The largest contribution in this category came from uncertainty in the K_L momentum spectrum employed as an input to the various MC studies. It affected both acceptance and efficiency, and resulted in the fractional uncertainty of 4.8% in the final branching ratio. The second largest contribution stemmed from uncertainty in the matrix element of the theoretical model. This brought 3.9% uncertainty in the acceptance ratio. The second category is related to the number of the events $N(\pi^+ \pi^- e^+ e^-)$ and/or $N(\pi^+ \pi^- \pi_D^0)$. We checked stability of the background subtraction by employing different control regions. Actually, widening the region in the $M_{\pi\pi ee}$ direction, we tried $|M_{\pi\pi ee} - M_{K_L}| < 5\sigma_{M_{K_L}}$ and $< 7\sigma_{M_{K_L}}$ instead of $< 3\sigma_{M_{K_L}}$. We considered the biggest difference resulted from this treatment as a systematic error (7.4%). For the He data, we also tested different event shapes assumed for the backgrounds due to the nuclear interaction. The effect was at most 3.6% as long as they gave statistically consistent results with the null observation. All other background contaminations, such as external γ -ray conversion events associated with $K_L \rightarrow \pi^+ \pi^- \gamma$ and $K_L \rightarrow \pi^+ \pi^- \pi^0$ ($\pi^0 \rightarrow \gamma\gamma$), were estimated to be small (1.4%). The final category is related to the current experimental errors on the branching ratios $Br(K_L \rightarrow \pi^+ \pi^- \pi^0)$ and $Br(\pi^0 \rightarrow e^+ e^- \gamma)$. Summing up all the uncertainties in quadrature, we found the over all systematic error to be 11.3%.

In summary, we observed 13.5 ± 4.0 $K_L \rightarrow \pi^+ \pi^- e^+ e^-$ events, and determined its branching ratio to be $(4.4 \pm 1.3(\text{stat.}) \pm 0.5(\text{syst.})) \times 10^{-7}$. The result is found to agree with the theoretical prediction as well as the recent measurement.

Acknowledgements

We wish to thank Professors H. Sugawara, S. Yamada, S. Iwata, K. Nakai, and K. Nakamura for their support and encouragement. We also acknowledge the support from the operating crew of the Proton Synchrotron, the members of Beam Channel group, Computing Center and Mechanical Engineering Center at KEK. Y.T, Y.M and M.S acknowledge receipt of Research Fellowships of the Japan Society for the Promotion of Science for Young Scientists.

References

- [1] T. Nomura *et al.*, Phys. Lett. B **408**, 445 (1997)
- [2] L. M. Sehgal and M. Wanninger, Phys. Rev. D**46**, 1035 (1992); **46**, 5209(E)(1992); P. Heilinger and L. M. Sehgal, *ibid.* **48**, 4146 (1993).
- [3] D. P. Majumdar and J. Smith, Phys. Rev. **187**, 2039 (1969); J. K. Elwood *et al.*, Phys. Rev. D**52**, 5095 (1995); J. K. Elwood *et al.*, *ibid.* **53**, 4078 (1996).
- [4] J.Adams *et al.*, Phys. Rev. Lett. **80**, 4123 (1998)
- [5] Preliminary results were presented at the SLAC topical conference; see N. Sasao, Proceedings of the SLAC topical conference (Aug. 1997).
- [6] Out of this, 2066 events came from the He data, which is different from the one presented in Ref. [1]. This is because some of the applied cuts, in particular those related to track/vertex quality, were tightened to further reduce backgrounds.
- [7] We have changed slightly the definition of χ_D^2 : the third term is now quadratic in θ . The change does not alter any results, and makes the interpretation of χ_D^2 more transparent statistically.
- [8] The standard deviation σ_θ was determined as follows. We could define the quantity θ as $\theta = \sqrt{\theta_{x'}^2 + \theta_{y'}^2}$, where $\theta_{x'}$ and $\theta_{y'}$ are projected angles onto some mutually orthogonal planes containing the target and vertex point. It was found that $\theta_{x'}$ and $\theta_{y'}$ were expressed by a Gauss distribution function with an approximately equal r.m.s. deviation of $\sigma_\theta \simeq 1.2$ mrad.
- [9] We checked statistical consistency of the two data sets: one observing 15 events (including backgrounds) and the other none. The probability was found to be $\sim 6\%$, which is somewhat small but not unreasonable.
- [10] Apparent change in the acceptance values from those quoted in Ref. [1] is not essential and has occurred as follows. In the acceptance/efficiency calculations, the cut imposed on M_{ee} , which previously had been applied in acceptance, was treated in efficiency. In addition, we used measured K_L Dalitz plot parameters [11] to calculate the $\pi^+\pi^-\pi^0$ matrix element instead of phase space.
- [11] Particle Data Group, C. Caso *et al.*, Eur. Phys. J. **C3**, 1-794 (1998)